

1 Artificial neuronal networks (ANN) to model the hydrolysis of 2 goat milk protein by subtilisin and trypsin

3 **Short title:** ANN modelling of the hydrolysis of goat milk protein

4

5 F. Javier Espejo-Carpio, Raúl Pérez-Gálvez*, Antonio Guadix, Emilia M. Guadix

6 Department of Chemical Engineering, University of Granada, 18071 Granada, Spain

7 **SUMMARY**

8 The enzymatic hydrolysis of milk proteins yield final products with improved properties and
9 reduced allergenicity. The degree of hydrolysis (DH) influences both technological (e.g., solubility,
10 water binding capacity) and biological (e.g., Angiotensin-converting enzyme (ACE) inhibition,
11 antioxidation) properties of the resulting hydrolysate. Phenomenological models are unable to
12 reproduce the complexity of enzymatic reactions in dairy systems. However, empirical approaches
13 offer high predictability and can be easily transposed to different substrates and enzymes. In this
14 work, the DH of goat milk protein by subtilisin and trypsin was modelled by feedforward artificial
15 neural networks (ANN). To this end, we produced a set of protein hydrolysates, employing various
16 reaction temperatures and enzyme/substrate ratios, based on an experimental design

17 The time evolution of the DH was monitored and processed to generate the ANN models. Extensive
18 hydrolysis is desirable because a high DH enhances some bioactivities in the final hydrolysate, such
19 as antioxidant or antihypertensive. The optimisation of both ANN models led to a maximal DH of
20 23.47% at 56.4°C and enzyme-substrate ratio of 5% for subtilisin, while hydrolysis with trypsin
21 reached a maximum of 21.3% at 35°C and an enzyme-substrate ratio of 4%.

22

23 **Keywords:** enzymatic hydrolysis; goat milk hydrolysates; artificial neural networks; proteases;
24 optimization

* Corresponding author: Tel.: +34 958 240532; Fax: +34 958 248992; Email: rperezga@ugr.es

25 **1. INTRODUCTION**

26 Enzymatic hydrolysis of proteins is an important process in the food industry that improves the
27 functional properties of proteins, reduces potential allergenicity and releases peptides displaying a
28 number of biological activities (Tavano, 2013). Food protein hydrolysates present improved
29 properties such as solubility, emulsifying capacity, foaming ability, water or oil holding capacities,
30 related to crude proteins (García-Moreno et al., 2016; Muro Urista et al., 2011). Moreover, these
31 can be incorporated into nutraceutical formulations where they exert certain biological reactions,
32 including antimicrobial, antioxidant and antihypertensive activities (Capriotti et al., 2016). Among a
33 wide range of substrates, cow milk protein hydrolysates have been the subject of extensive research,
34 while goat milk protein hydrolysates have only recently been shown to exhibit functional and
35 bioactive properties (Bernacka, 2011; El-Salam and El-Shibiny, 2013). Serine endopeptidases, such
36 as subtilisin and trypsin, are usually employed in the hydrolysis of food proteins. Particularly, while
37 subtilisin is able to attack a wide range of peptide bonds, trypsin preferentially cleaves at arginine
38 and lysine residues. Both enzymes have been used for producing peptides displaying biological
39 activities such as antioxidant (Pihlanto, 2006), antihypertensive (López-Fandiño et al., 2006) or
40 antimicrobial (Gobbetti et al., 2004). Moreover, these enzymes yield protein hydrolysates with
41 improved technological properties such as solubility, emulsifying and foaming capacity (Severin
42 and Xia, 2006; Van der Ven et al., 2001).

43 Many functional and biological properties of protein hydrolysates are related to their degree of
44 hydrolysis (DH). For example, emulsifying and foaming capacities present a maximum at a specific
45 degree of hydrolysis, and, if this is exceeded, these properties are reduced (de Castro et al., 2015).
46 An extensive DH exerts a positive effect on antihypertensive activity because most of the active
47 peptides have chain lengths shorter than 12 amino acids (Li et al., 2004; Phelan and Kerins, 2011).
48 Similarly, extensive hydrolysis of milk proteins can reduce allergenicity significantly for use in
49 infant formulas (Duan et al., 2014; Dupont et al., 2015) .

50 It can be concluded the extent of the hydrolysis reaction is a key parameter which should be
51 controlled and predicted accurately to obtain hydrolysates with specific characteristics. Mechanistic
52 approaches fail to describe the complexity of various proteins present in milk and different reactions
53 that occurs during milk hydrolysis (e.g., product inhibition, enzyme thermal denaturation)(Ba and
54 Boyaci, 2007). In this context, methods based on direct analysis of experimental data using
55 response surfaces or artificial neural networks, are a suitable alternative to those based on
56 phenomenological hypotheses. These empirical methods are applicable to all types of enzymatic
57 reactions and do not require kinetic assumptions (Baş et al., 2007).

58 In particular, response surface methodology is widely used for modelling and optimisation
59 purposes, for which the response of interest is influenced by several variables. However, this
60 method is limited in most cases by the use of polynomial equations. Instead, ANNs can be used to
61 ensure better data fit and estimation capabilities (Ba and Boyaci, 2007; Fatiha et al., 2013) .

62 ANN is composed of individual processing elements (i.e., neurons) that transform weighted input
63 variables into an output by means of an activation function. ANNs comprise one or more hidden
64 layers of neurons. A key element of this approach is the training algorithm, which allows to update
65 the weights and biases of the neurons to obtain outputs closer to the targets. This training consists of
66 minimizing the average squared error (MSE) between the calculated values and the experimental
67 data.

68 The ANNs have been successfully employed for modelling enzymatic reactions. For example,
69 Bryjak et al. (2000) applied ANNs to model starch hydrolysis by glucoamylase, while Bas et al.
70 (2007) studied the reaction rates of maltose hydrolysis by amyloglucosidase. As for the protein
71 hydrolysis, Abakarov et al. (2011) satisfactorily modelled the kinetics of enzymatic hydrolysis of
72 squid protein with subtilisin using the reaction time and the substrate concentration as input
73 variables. Bucinski et al. (2008) and Li et al. (2016) evaluated the variation of DH during the
74 hydrolysis of bovine hemoglobin and pea proteins, respectively. Li et al. (2006) developed a
75 predictive model for the production of antioxidant peptides from fish proteins taking into account a
76 number of input variables such as pH, temperature, hydrolysis time, muscle/water ratio and
77 enzyme/substrate ratio. Regarding milk proteins, Pinto et al. (2007) proposed a hybrid neural-
78 kinetic model for predicting the molecular mass distribution of whey protein hydrolysates.

79 The aim of this study was to develop two ANN models for the enzymatic hydrolysis of goat milk
80 proteins, employing either subtilisin or trypsin as catalysts. For each model, the DH was modelled
81 as a function of temperature, enzyme-substrate ratio and the reaction time. Firstly, the architecture
82 of the neural network (i.e., number of neurons in the hidden layer) and the training algorithm were
83 chosen to maximise the degree of fitness (i.e., mean squared error) of the model. Both ANN models
84 were then optimised for the maximal DH, which is desirable because it improves ACE inhibitory
85 and antioxidant activities of the resulting hydrolysates.

86 **2. MATERIALS AND METHODS**

87 **2.1. Materials**

88 Commercial UHT goat milk (33 g protein/L) was purchased from local store. The enzymes used for
89 the assays were subtilisin (EC 3.4.21.62) and trypsin (EC 3.4.21.4), both supplied by Novozymes
90 (Denmark).

91 **2.2. Enzymatic reaction and determination of the degree of hydrolysis**

92 Before hydrolysis, the milk was skimmed by centrifugation at 4 °C and 5000 g for 20 min in a
93 Sigma 6k15 centrifuge (Sigma Laborzentrifugen, Germany). Skimmed goat milk (200 mL) was
94 then hydrolysed in a stirred tank reactor for 5 hours. Initially, the pH of the milk was set at pH 8
95 with 1M NaOH. After reaching the desired temperature, the enzyme was added at different enzyme-
96 substrate ratio. In alkaline medium, the cleavage of peptide bonds releases protons which cause the
97 pH to drop. An automatic titrator was employed (718 Stat Titrimo, Metrohm, Switzerland) to keep
98 the pH constant during the reaction by adding NaOH (1M). The degree of hydrolysis (DH), defined
99 as the percentage of available peptide bonds which are cleaved during the reaction, can be related to
100 the amount of base consumed by Eq. 1 (Adler Nissen, 1986):

$$101 \quad DH = n_B / (\alpha \cdot m_P \cdot h_{TOT}) \quad (1)$$

102 where DH is the degree of hydrolysis, n_B (mol) is the amount of NaOH consumed to keep the pH
103 constant, α is the average degree of dissociation of α -NH₂ groups released during hydrolysis, m_P =
104 6.6 g is the mass of protein in the substrate and h_{TOT} = 0.0082 eq/g is the average number of
105 equivalents of peptide bonds per gram of casein protein.

106 **2.3. Experimental design**

107 A total of 60 hydrolysates were produced, broken down into two factorial designs of 30 experiments
108 where subtilisin or trypsin were employed as catalysts. Each hydrolysate was produced at a given
109 combination of reaction temperature (T) and enzyme-substrate ratio (ES), which were the input
110 variables of the factorial designs. The reaction temperature was varied at six levels according to the
111 thermal stability of the enzyme assayed. Subtilisin exhibits wide thermal stability, presenting
112 optimal activity around 50-55°C. As for trypsin, it presents maximal activity around 40°C (Adler
113 Nissen, 1986). Therefore, subtilisin was tested at 45, 50, 55, 60, 65 and 70 °C, while trypsin was at
114 30, 35, 40, 45, 50 and 55 °C. The levels assayed for the enzyme to substrate ratio were 1, 2, 3, 4 and
115 5 % for both enzymes. As for the time of reaction (t), the DH value was recorded every 60 seconds
116 over the course of the reaction (5 hours). This yields an amount of 300 experimental data (T, ES, t,
117 DH) for each hydrolysis curve.

118

119

120 **2.3. Structure and training of the artificial neuronal network**

121 Two artificial neural network (ANN) models were developed in this work (i.e. subtilisin and
122 trypsin), where DH was related to the reaction temperature (T), the enzyme-substrate ratio (ES) and
123 the time of reaction (t) as input variables. Both ANN models were constructed by means of the
124 Neural Network Toolbox, implemented in Matlab 7.0 (Mathworks, USA).

125 Both artificial neural networks comprised an input layer, a single hidden layer and an output layer.
126 The input layer comprised three neurons, corresponding to the 3 input variables (T, ES, t). This
127 layer is connected to the hidden layer, whose number of neurons was varied from 1 to 10 neurons.
128 Each neuron k of the hidden layer received a weighted signal from the input layer s_k , expressed as
129 follows:

$$130 \quad s_k = \sum_{i=1}^3 w_{ik} \cdot X_i + b_k \quad (2)$$

131 where w_{ik} were the weight factors and b_k was the bias for the neuron k . Each neuron of the hidden
132 layer processes the signal s_k by means of a transfer function. The sigmoid function (implemented in
133 Matlab as *logsig*) was selected as transfer function in the hidden layer, which returns a value
134 ranging between 0 and 1 according to Eq. 3:

$$135 \quad \text{logsig}(s_k) = \frac{1}{1 + \exp(-s_k)} \quad (3)$$

136 The k responses exiting the hidden layer are combined into a single weighted signal t , which is
137 received by an output neuron, which returns the predicted value of DH. The saturated symmetric
138 lineal function was chosen as transfer function for the output layer. This function truncates the
139 weighted signal t within the interval [0,1], avoiding either negative DH values or above 1.

140 Three training algorithms were tested in this work: gradient descent with momentum
141 backpropagation (*traingdm*), resilient backpropagation (*trainrp*) and Levenberg-Marquardt
142 backpropagation (*trainlm*). These algorithms update the weight and bias values in order to minimize
143 the mean squared error (MSE) between observed and predicted DH.

144 For a fixed number of hidden neurons in the hidden layer and training algorithm (*traingdm*, *trainrp*
145 and *trainlm*), 30 runs were carried, ensuring an appropriate population of predicted data. At the
146 beginning of each run, the dataset was normalized and then randomly divided into three subsets:

147 training, validation and test. The biggest subset (70 % of the total amount of experimental data) was
148 used for training the network using the algorithm selected. During the training, the error obtained
149 from the validation set (15% of the data) was employed for early stopping (i.e. interruption of the
150 iteration process when over-fitting in the training dataset is detected). In back-propagation methods,
151 over-fitting occurs when an improvement in the fit of the training data is accompanied by larger
152 generalization errors. The number of iterations per training run was limited to 10000. As an early
153 stopping criterion, the training process stopped when the MSE increased for 10 iterations. At this
154 point, the algorithm returned the weights and biases corresponding to the minimal MSE recorded so
155 far. Finally, the remaining data (15%) are employed to compute the test error, which assesses the
156 predictive capability of the network. This error is also useful to know if a good division of the data
157 set (i.e. training, validation and evaluation subset) has been done.

158 **2.4. ANN model for DH and optimization procedure**

159 The objective of the ANN procedure was to obtain a predictive model of DH for each of the
160 enzymes employed. Each model allowed the calculation of DH as a function of the experimental
161 conditions of temperature, enzyme-substrate ratio and time of reaction, as expressed by Eq. 4:

$$162 \quad DH = \sum_{k=1}^N \omega_k \cdot \text{logsig} \left(\sum_{i=1}^3 w_{ki} \cdot X_i + b_k \right) + \beta \quad (4)$$

163 X (T, eS, t) denotes the vector of input variables (i.e, the experimental conditions for each
164 hydrolysis assay); w_{ki} and b_k are the weight factors and bias of the input layer, respectively; ω and
165 β are the weights and bias of the hidden layer and the transfer function logsig was defined by Eq. 3.

166 The training procedure allowed the estimation of the set of parameters w_k , b_k , ω and β yielding the
167 minimal squared error between predicted and observed DH (i.e., the best fit between the
168 experimental DH and the predictive model).

169 The goal of the optimisation problem was to find the set of experimental conditions X (T, eS, t),
170 within their experimental range, which maximises DH calculated by Eq. 4. To this end, the
171 Generalized Reduced Gradient (GRG), implemented in the Solver tool of the MS Excel, was chosen
172 for the optimization of both models. GRG is a non-linear optimisation algorithm, which basically
173 evaluates the gradient or slope of the objective function (i.e. predicted DH) as the input values (i.e.
174 experimental conditions X_i in Eq. 4) change and determines that it has reached an optimum solution
175 when the partial derivatives equal zero. Since GRP is a local method, the multistart method was
176 chosen to find a globally optimal solution of the problem. This option consists in operating the GRP

177 algorithm from a set of starting points, reaching different local optimums which are then compared
178 to select a global optimum.

179 3. RESULTS AND DISCUSSION

180 3.1. Architecture and training algorithm of the ANN

181 The time evolution of the DH was modeled by two artificial neural networks, depending on the
182 enzyme employed for the hydrolysis. Each ANN comprised an input layer of three neurons
183 corresponding to each one of the experimental factors (T, ES, t), connected to a hidden layer with a
184 variable number of neurons between 1 and 10. The hidden layer is connected to an output layer with
185 a single neuron, which returns the predicted value for the degree of hydrolysis. An average of 30
186 simulations was performed by a combination of three training algorithms (i.e. *trainrp*, *traingdp*,
187 *trainlm*) and a fixed number of neurons in the hidden layer (i.e. 1 to 10). Every training procedure
188 was executed 30 times, starting from different initial values of weights and biases. For each trial,
189 the mean squared errors of the training, validation and test subsets were recorded. Average training
190 and validation errors were in all cases very similar to test error values. Indeed, the differences
191 between these errors were below 1 and 2 % for subtilisin and trypsin networks, respectively. Fig. 1
192 presents the test error of the networks obtained for the hydrolysis with subtilisin (a) and trypsin (b)
193 as a function of the training algorithm and the number of neurons in the hidden layer. For both
194 ANN models, the Levenberg-Marquardt algorithm showed the best performance, followed by
195 *trainrp* and *traingdm*. Indeed, test errors decreased with an increasing number of neurons in the
196 hidden layer for the *trainlm* algorithm, resulting in final MSE values of and $5 \cdot 10^{-4}$ and 10^{-3} at 10
197 neurons for the subtilisin and tripsin network, respectively. Contrarily, the *traingdp* algorithm
198 presented overfitting above 6 neurons for both ANN models. According to these results, the
199 Levenberg-Marquardt training algorithm was chosen to model the degree of hydrolysis for both
200 enzymes.

201 The predictability of both ANN models and the *trainlm* algorithm was assessed by the slope and
202 intercept of the linear fit between predicted and observed values of DH (Fig. 2). Ideally, the slope
203 and the intercept should be 1 and 0, respectively. In the case of the subtilisin ANN, the network
204 with 2 neurons in the hidden layer led to an average slope (i.e. mean value from 30 trials) above
205 0.950, which increased up to 0.996 at 8 neurons. This value remained steady in 9 and 10 neurons.
206 The intercept value for the subtilisin ANN was $6 \cdot 10^{-3}$ at 2 neurons and decreased down to $4 \cdot 10^{-4}$ at
207 10 neurons. Similarly, the average slope and intercept values for the trypsin ANN increased and

208 decreased, respectively, with the number of neurons in the hidden layer. This model reached a
209 maximal slope of 0.984 and a minimal intercept of $2 \cdot 10^{-3}$ at 10 neurons.

210 In line of the above, two ANN models were proposed to fit the experimental data employing the
211 Levenberg-Marquardt training algorithm. The number of neurons in the hidden layer was fixed at
212 8 and 10 for the subtilisin and trypsin ANN, respectively. Under these conditions, the predictability
213 of both models (i.e. MSE and slope values) was acceptable while their complexity and time of
214 computation were limited. This algorithm has been successfully employed to model enzymatic
215 processes. For example, Pinto et al. (2007) modeled the molecular weight distribution of whey
216 protein hydrolysates. Feed-forward ANNs trained by the Levensberg-Marquardt algorithm was used
217 to model the time evolution of DH in the hydrolysis of blood protein (Gálvez et al., 2016) and horse
218 mackerel protein (Morales-Medina et al., 2016) with subtilisin. Abakarov et al. (2011) used gradient
219 descent algorithm to predict the hydrolysis of squid protein using subtilisin. Similarly, Buciński et
220 al. (2008) use it for hydrolysis of pea protein employing trypsin.

221 **3.2. ANN models for the hydrolysis with subtilisin and trypsin**

222 In all the cases, the time evolution of DH followed the characteristic curve described for enzymatic
223 hydrolysis. As an example, Figures 3a and 3b represent the observed values of DH (point markers)
224 against the time of reaction and enzyme-substrate ratio for subtilisin and trypsin at 50°C. It can be
225 observed that DH presented a sharp linear increase at the beginning of the hydrolysis, followed by
226 slight reduction to achieve steady state. As the proteolysis progresses, the remaining number of
227 peptide bonds available for enzyme attack decreases and so the reaction rate. (Adler Nissen, 1986;
228 Valencia et al., 2014). Depending on its thermal stability, extensive times of reaction at high
229 temperatures may provoke thermal inactivation of the enzyme. The denaturation of the quaternary
230 structure of the enzyme results in a decrease of its enzymatic activity. Finally, some authors such as
231 Valencia et al. (2014) relate the decrease of the reaction rate to the occurrence of product inhibition.
232 In this case, the peptides released during hydrolysis may inhibit the reaction progress by forming
233 stable complexes with substrate or enzyme.

234 The hydrolysis curves depicted in Figure 3 show that increasing enzyme-substrate ratios improved
235 the final values of DH for the subtilisin reaction. This trend was not clear for the trypsin reactions,
236 where hydrolysis curves at ES 4% and 5% were very close or even overlapped with each other.

237 As example, at 50 °C, the final DH values observed for subtilisin and trypsin were in the range of
238 18-24%, and 16-23%, respectively. The solid lines in Figure 3 represent the predicted DH
239 calculated from the ANN models presented above. Figure 3 illustrates the high degree of fitting

240 between the observed values of DH and those calculated by ANN modelling. The determination
241 coefficients of the linear fit between experimental and calculated values of DH were $r^2=0.996$ and
242 $r^2=0.994$ for subtilisin and trypsin, respectively.

243

244

245 **3.3. Optimization of the degree of hydrolysis**

246 The application of the Levensberg-Marquardt algorithm allowed estimating the weights and biases
247 of both ANN models (Eq. 2) for a fixed number of neurons in the hidden layer. This set of
248 parameters allowed computing DH as a function of the reaction conditions (i.e. T, ES and t).
249 Furthermore, these model were optimized by an evolutionary algorithm to determine the optimal
250 parameters for maximal DH. Extensive hydrolysis seems to enhance a number of biological
251 activities such as the ACE-inhibitory and the antioxidant activities. Some of the most potent ACE
252 inhibitors identified in milk protein hydrolysates correspond to di and tripeptides (Hernández-
253 Ledesma et al., 2014). Similarly, several short peptides (500-1800 Da) have been identified as
254 potent antioxidants (Ahmed et al., 2015; Moreno-Montoro et al., 2017; Samaranayaka and Li-Chan,
255 2011). Peptide size is also a crucial factor for bioavailability of bioactive peptides. According to the
256 literature, there are no evidence that peptides bigger than tripeptides can move across the tissues of
257 gastrointestinal tract intact and enter into blood stream in required concentrations (Miner-Williams
258 et al., 2014). The contour plots shown in Figures 4a and 4b represent the calculated values of the
259 final DH (5 h) against the reaction temperature and the enzyme-substrate ratio. Both contour plots
260 confirm the positive effect of increasing enzyme-substrate ratio on DH. This trend was clear for the
261 hydrolysis with subtilisin, regardless the reaction temperature. Increasing ES ratios favoured the
262 proteolysis with subtilisin, obtaining maximum DH of 22 – 23% with 5% ES ratio. Optimisation
263 of the ANN model confirmed that maximum DH (23.47%) can be achieved for goat milk proteins
264 using subtilisin at 56.4 °C with 5% ES ratio. The optimal reaction temperature is within the range
265 of maximal activity reported for subtilisin (Adler Nissen, 1986; Ma et al., 2015). According to the
266 contour plot, the final values of DH at 5% ES ratio kept above 22% within the experimental range
267 from 45 to 70°C. This suggests that this enzyme was not significantly affected by thermal
268 deactivation, and therefore its proteolytic activity remained unaltered. This is in line with previous
269 studies which highlight the high resistance of subtilisin against thermal denaturation (Adler-Nissen,
270 1986; Nagodawithana and Reed, 2013). Subtilisin-like serine proteases contain a variable number (2
271 to 7) of Ca^{2+} -binding sites. Binding of the calcium ions has been reported to greatly stabilise the
272 protein structure against thermal unfolding (Foophow et al., 2010).

273 In contrast, the contour plots for the hydrolysis with trypsin (Figure 4b) indicated that the final DH
274 was influenced by the reaction temperature. This may resulted from inactivation of trypsin at higher
275 temperature. The optimal conditions for maximal DH (21.3%) were 35°C and ES 4%. Higher levels
276 of enzyme-substrate ratio did not improve the extent of the hydrolysis, suggesting the saturation of
277 the peptide bonds available. Trypsin exhibits narrow specificity towards arginine and lysine
278 residues (Olsen et al., 2004) , while subtilisin is a wide-spectrum protease. This fact could explain
279 the saturation of available peptide bonds at ES ratios above 4%. The optimal temperature condition
280 calculated for trypsin was 35°C, similar to the maximum of 37°C reported in scientific literature
281 (Adler-Nissen, 1986; Morales-Medina et al., 2016).

282 For validation purposes, the optimal operating conditions for maximal DH were reproduced
283 experimentally for both enzymes. To this end, the predicted optimum conditions for both subtilisin
284 (56.4 °C and ES 5%) and trypsin (35 °C and ES 4%) were experimentally evaluated and illustrated
285 in the Figure 5. Some of the observed values of DH were represented by point markers, while the
286 curves predicted from the ANN model were depicted as solid lines. Both curves fitted satisfactorily
287 the observed data. This was confirmed by the coefficients of determination R^2 for both models,
288 which were 0.9883 and 0.9929 for subtilisin and trypsin, respectively. Moreover, the average
289 deviation between observed and predicted values was 1.9 ± 1.7 % for the hydrolysis with subtilisin
290 and 1.7 ± 1.6 % for trypsin. The verification hydrolysis with subtilisin led to a maximal DH of
291 23.26% at experimental conditions 56.4°C, 5% ES ratio and 5 h of reaction, which was similar to
292 the optimum DH (23.47%, 56.4°C, 5% ES ratio, 5 h) predicted by the proposed ANN model with 8
293 neurons in the hidden layer. However, maximum DH obtained for trypsin mediated hydrolysis
294 under experimental conditions (35°C, 4% ES ratio and 5 h of reaction) was 22.17%, which is
295 slightly higher than the predicted value (21.3%) with optimum conditions (35 °C, ES 4% and 5 h)
296 using the ANN model with 10 neurons.

297 **4. CONCLUSIONS**

298 ANN modelling was successfully employed to predict the degree of hydrolysis of skimmed goat
299 milk proteins with subtilisin and trypsin as a function of the operating conditions, namely the
300 reaction temperature, the enzyme-substrate ratio and the time of hydrolysis. The predictability of
301 both ANN models was improved by testing three training algorithm and a variable number of
302 neurons (i.e. 1 to 10) in the hidden layer. In this regard, two ANN models with 8 and 10 neurons in
303 the hidden layer were selected for subtilisin and trypsin hydrolysis, respectively. As for the training
304 algorithm, the Levenberg-Marquardt led to the minimal test errors (MSE) for both subtilisin and

305 trypsin with determination coefficients of 0.996 and 0.984, respectively. Furthermore, these models
306 were optimized by an evolutionary algorithm to obtain the combination of operating conditions
307 leading to the maximal DH. Maximum DH (23.47%) was calculated for subtilisin at 56.4 °C, ES
308 5% and 5 h of reaction, while the maximum DH obtained for trypsin was 21.3% at 35 °C, ES 4%
309 and 5 h reaction. There was a significant correlation between DH predicted using ANN models and
310 DH obtained under experimental conditions.

311 ANN arises as an alternative to obtain predictive models for protein hydrolysis, especially when a
312 large volume of data is available. The strength of these models, inspired in human brain, lies on its
313 ability to learn from experimental data by training algorithms. By this approach, the model
314 parameters are updated iteratively, until minimizing the error between predicted and actual data. In
315 the field of biochemical processes, this approach allows obtaining predictive models without
316 needing to have extensive knowledge of the underlying mechanism. This is especially useful in
317 enzymatic reactions where several phenomena (i.e. substrate solubilisation, substrate or product
318 inhibition, thermal inactivation of the enzyme) may occur simultaneously.

319 **Acknowledgments**

320 This work was funded by the project P07-TEP-02579 from the Consejería de Economía,
321 Innovación, Ciencia y Empleo of Junta de Andalucía, Spain.

322

323 **REFERENCES**

- 324 Abakarov, A., Teixeira, A., Simpson, R., Pinto, M., Almonacid, S., 2011. Modeling of Squid
325 Protein Hydrolysis: Artificial Neural Network Approach. *Journal of Food Process Engineering*
326 34, 2026–2046. doi:10.1111/j.1745-4530.2009.00567.x
- 327 Adamson, N.J., Reynolds, E.C., 1996. Characterization of casein phosphopeptides prepared using
328 alcalase: Determination of enzyme specificity. *Enzyme and Microbial Technology* 19, 202–
329 207. doi:10.1016/0141-0229(95)00232-4
- 330 Adler Nissen, 1986. *Enzymic hydrolysis of food proteins*. Elsevier Applied Science Publishers
331 LTD, London.
- 332 Ahmed, A.S., El-Bassiony, T., Elmalt, L.M., Ibrahim, H.R., 2015. Identification of potent
333 antioxidant bioactive peptides from goat milk proteins. *Food Research International* 74, 80–88.
334 doi:10.1016/j.foodres.2015.04.032
- 335 Ba, D., Boyaci, I.H., 2007. Modeling and optimization II: Comparison of estimation capabilities of
336 response surface methodology with artificial neural networks in a biochemical reaction.
337 *Journal of Food Engineering* 78, 846–854. doi:10.1016/j.jfoodeng.2005.11.025
- 338 Baş, D., Dudak, F.C., Boyacı, İ.H., 2007. Modeling and optimization III: Reaction rate estimation
339 using artificial neural network (ANN) without a kinetic model. *Journal of Food Engineering*
340 79, 622–628. doi:10.1016/j.jfoodeng.2006.02.021
- 341 Bernacka, H., 2011. Health-promoting properties of goat milk. *Medycyna Weterynaryjna* 67.
- 342 Bryjak, J., Murlikiewicz, K., Zbiciński, I., Stawczyk, J., 2000. Application of artificial neural
343 networks to modelling of starch hydrolysis by glucoamylase. *Bioprocess Engineering* 23.
344 doi:10.1007/s004499900170
- 345 Buciniński, A., Karamać, M., Amarowicz, R., Pegg, R.B., 2008. Modeling the tryptic hydrolysis of
346 pea proteins using an artificial neural network. *LWT - Food Science and Technology* 41, 942–
347 945. doi:10.1016/j.lwt.2007.06.021
- 348 Capriotti, A.L., Cavaliere, C., Piovesana, S., Samperi, R., Laganà, A., 2016. Recent trends in the
349 analysis of bioactive peptides in milk and dairy products. *Analytical and Bioanalytical*
350 *Chemistry* 408. doi:10.1007/s00216-016-9303-8
- 351 de Castro, R.J.S., Bagagli, M.P., Sato, H.H., 2015. Improving the functional properties of milk
352 proteins: Focus on the specificities of proteolytic enzymes. *Current Opinion in Food Science* 1,
353 64–69. doi:10.1016/j.cofs.2014.12.004

- 354 Duan, C.-C., Yang, L.-J., Li, A.-L., Zhao, R., Huo, G.-C., 2014. Effects of enzymatic hydrolysis on
355 the allergenicity of whey protein concentrates. *Iranian Journal of Allergy, Asthma and*
356 *Immunology* 13.
- 357 Dupont, C., Hol, J., Nieuwenhuis, E.E.S., De Jongste, J.C., Samsom, J.N., Van Leer, E.H.G., Elink
358 Schuurman, B.E.E., De Ruiter, L.F., Neijens, H.J., Versteegh, F.G.A., Groeneweg, M., Van
359 Veen, L.N., Vaessen-Verberne, A.A., Smit, M.J.M., Vriesman, A.W., Roosen, Y.M., Den
360 Exter, G.L., 2015. An extensively hydrolysed casein-based formula for infants with cows' milk
361 protein allergy: Tolerance/hypo-allergenicity and growth catch-up. *British Journal of Nutrition*
362 113. doi:10.1017/S000711451500015X
- 363 El-Salam, M.H.A., El-Shibiny, S., 2013. Bioactive Peptides of Buffalo, Camel, Goat, Sheep, Mare,
364 and Yak Milks and Milk Products. *Food Reviews International* 29, 1–23.
365 doi:10.1080/87559129.2012.692137
- 366 Fatiha, B., Sameh, B., Youcef, S., Zeineddine, D., Nacer, R., 2013. Comparison of artificial neural
367 network (ANN) and response surface methodology (RSM) in optimization of the
368 immobilization conditions for lipase from *Candida rugosa* on amberjet® 4200-Cl. *Preparative*
369 *Biochemistry and Biotechnology* 43. doi:10.1080/10826068.2012.693899
- 370 Foophow, T., Foophow, T., Tanaka, S., Koga, Y., Takano, K., Kanaya, S., 2010. Subtilisin-like
371 serine protease from hyperthermophilic archaeon *Thermococcus kodakaraensis* with N- and C-
372 terminal propeptides. *Protein Engineering, Design and Selection* 23, 347–355.
373 doi:10.1093/protein/gzp092
- 374 Gálvez, R.P., Carpio, F.J.E., Guadix, E.M., Guadix, A., 2016. Artificial neural networks to model
375 the production of blood protein hydrolysates for plant fertilisation. *Journal of the Science of*
376 *Food and Agriculture* 96. doi:10.1002/jsfa.7083
- 377 García-Moreno, P.J., Pérez-Gálvez, R., Espejo-Carpio, F.J., Ruiz-Quesada, C., Pérez-Morilla, A.I.,
378 Martínez-Agustín, O., Guadix, A., Guadix, E.M., 2016. Functional, bioactive and antigenicity
379 properties of blue whiting protein hydrolysates: Effect of enzymatic treatment and degree of
380 hydrolysis. *Journal of the Science of Food and Agriculture*. doi:10.1002/jsfa.7731
- 381 Geerlings, A., Villar, I.C., Zarco, F.H., Sánchez, M., Vera, R., Gomez, A.Z., Boza, J., Duarte, J.,
382 2006. Identification and characterization of novel angiotensin-converting enzyme inhibitors
383 obtained from goat milk. *Journal of Dairy Science* 89.
- 384 Gobbetti, M., Minervini, F., Rizzello, C.G., 2004. Angiotensin I-converting-enzyme-inhibitory and
385 antimicrobial bioactive peptides. *International Journal of Dairy Technology* 57.

- 386 doi:10.1111/j.1471-0307.2004.00139.x
- 387 Hernández-Ledesma, B., García-Nebot, M.J., Fernández-Tomé, S., Amigo, L., Recio, I., 2014.
388 Dairy protein hydrolysates: Peptides for health benefits. *International Dairy Journal* 38, 82–
389 100. doi:10.1016/j.idairyj.2013.11.004
- 390 Li, G.-H., Le, G.-W., Shi, Y.-H., Shrestha, S., 2004. Angiotensin I–converting enzyme inhibitory
391 peptides derived from food proteins and their physiological and pharmacological effects.
392 *Nutrition Research* 24, 469–486. doi:10.1016/j.nutres.2003.10.014
- 393 Li, L., Wang, J., Zhao, M., Cui, C., Jiang, Y., 2006. Artificial neural network for production of
394 antioxidant peptides derived from bighead carp muscles with alcalase. *Food Technology and*
395 *Biotechnology* 44, 441–448.
- 396 Li, S., Hu, Y., Hong, Y., Xu, L., Zhou, M., Fu, C., Wang, C., Xu, N., Li, D., 2016. Analysis of the
397 Hydrolytic Capacities of *Aspergillus oryzae* Proteases on Soybean Protein Using Artificial
398 Neural Networks. *Journal of Food Processing and Preservation* 40, 918–924.
399 doi:10.1111/jfpp.12670
- 400 López-Fandiño, R., Otte, J., van Camp, J., 2006. Physiological, chemical and technological aspects
401 of milk-protein-derived peptides with antihypertensive and ACE-inhibitory activity.
402 *International Dairy Journal* 16. doi:10.1016/j.idairyj.2006.06.004
- 403 Ma, Y., Sun, X., Wang, L., 2015. Study on optimal conditions of alcalase enzymatic hydrolysis of
404 soybean protein isolate. *Advance Journal of Food Science and Technology* 9, 154–158.
- 405 Miner-Williams, W.M., Stevens, B.R., Moughan, P.J., 2014. Are intact peptides absorbed from the
406 healthy gut in the adult human? *Nutrition Research Reviews* 27, 308–329.
407 doi:10.1017/S0954422414000225
- 408 Morales-Medina, R., Pérez-Gálvez, R., Guadix, A., Guadix, E.M., 2016. Artificial neuronal
409 network modeling of the enzymatic hydrolysis of horse mackerel protein using protease
410 mixtures. *Biochemical Engineering Journal* 105. doi:10.1016/j.bej.2015.10.009
- 411 Moreno-Montoro, M., Olalla-Herrera, M., Rufián-Henares, J.Á., Martínez, R.G., Miralles, B.,
412 Bergillos, T., Navarro-Alarcón, M., Jauregi, P., 2017. Antioxidant, ACE-inhibitory and
413 antimicrobial activity of fermented goat milk: Activity and physicochemical property
414 relationship of the peptide components. *Food and Function* 8, 2783–2791.
415 doi:10.1039/c7fo00666g
- 416 Muro Urista, C., Álvarez Fernández, R., Riera Rodríguez, F., Arana Cuenca, A., Téllez Jurado, A.,
417 2011. Review: Production and functionality of active peptides from milk. *Food Science and*

- 418 Technology International 17. doi:10.1177/1082013211398801
- 419 Nagodawithana, T., Reed, G., 2013. *Enzymes in Food Processing*. Elsevier.
- 420 Olsen, J. V, Ong, S.-E., Mann, M., 2004. Trypsin cleaves exclusively C-terminal to arginine and
421 lysine residues. *Molecular & cellular proteomics : MCP* 3, 608–14. doi:10.1074/mcp.T400003-
422 MCP200
- 423 Phelan, M., Kerins, D., 2011. The potential role of milk-derived peptides in cardiovascular disease.
424 *Food and Function* 2. doi:10.1039/c1fo10017c
- 425 Pihlanto, A., 2006. Antioxidative peptides derived from milk proteins. *International Dairy Journal*
426 16, 1306–1314. doi:10.1016/j.idairyj.2006.06.005
- 427 Pinto, G.A., Giordano, R.L.C., Giordano, R.C., 2007. Neural Network Inference of Molar Mass
428 Distributions of Peptides during Tailor-Made Enzymatic Hydrolysis of Cheese Whey: Effects
429 of pH and Temperature. *Applied Biochemistry and Biotechnology* 143, 142–152.
430 doi:10.1007/s12010-007-0039-y
- 431 Samaranayaka, A.G.P., Li-Chan, E.C.Y., 2011. Food-derived peptidic antioxidants: A review of
432 their production, assessment, and potential applications. *Journal of Functional Foods* 3, 229–
433 254. doi:10.1016/j.jff.2011.05.006
- 434 Severin, S., Xia, W.S., 2006. Enzymatic hydrolysis of whey proteins by two different proteases and
435 their effect on the functional properties of resulting protein hydrolysates. *Journal of Food*
436 *Biochemistry* 30. doi:10.1111/j.1745-4514.2005.00048.x
- 437 Tavano, O.L., 2013. Protein hydrolysis using proteases: An important tool for food biotechnology.
438 *Journal of Molecular Catalysis B: Enzymatic* 90, 1–11. doi:10.1016/j.molcatb.2013.01.011
- 439 Van der Ven, C., Gruppen, H., De Bont, D.B.A., Voragen, A.G.J., 2001. Emulsion properties of
440 casein and whey protein hydrolysates and the relation with other hydrolysate characteristics.
441 *Journal of Agricultural and Food Chemistry* 49, 5005–5012. doi:10.1021/jf010144c

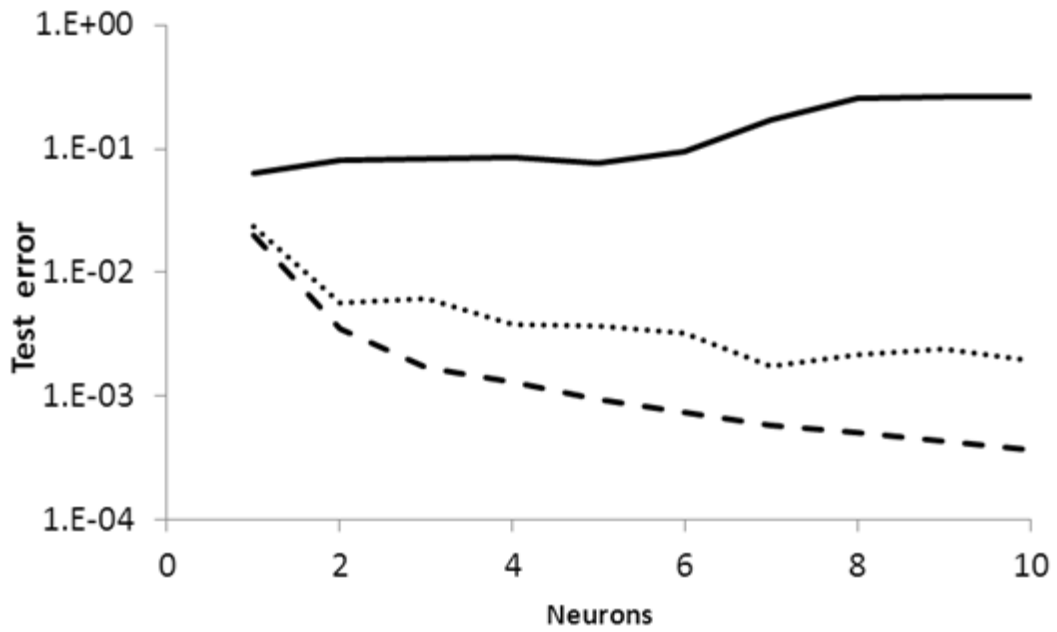
442

443

444

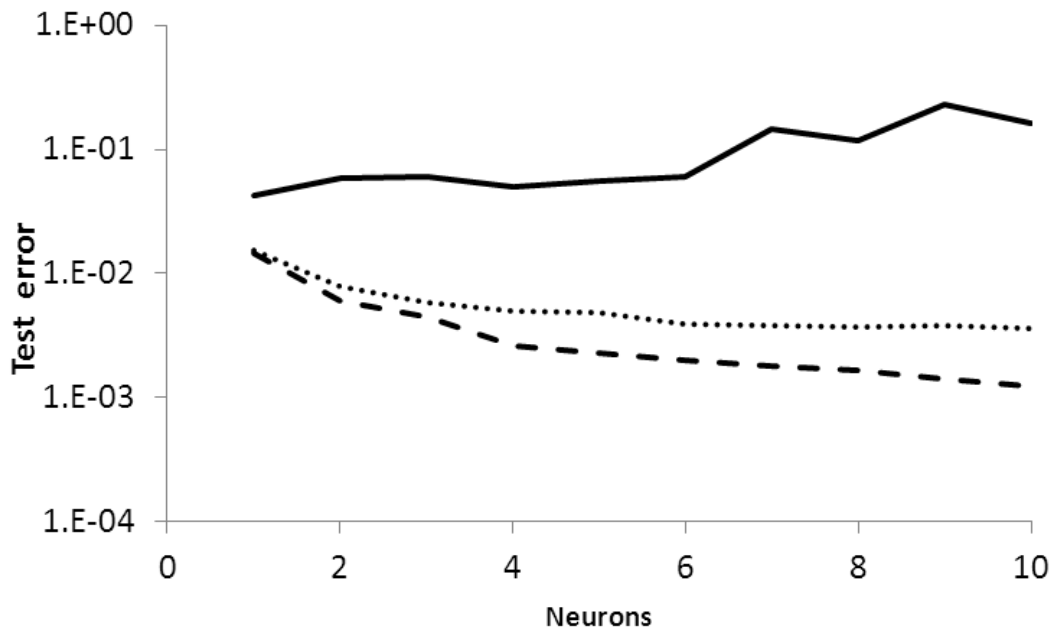
445

446 (a)



447

448 (b)

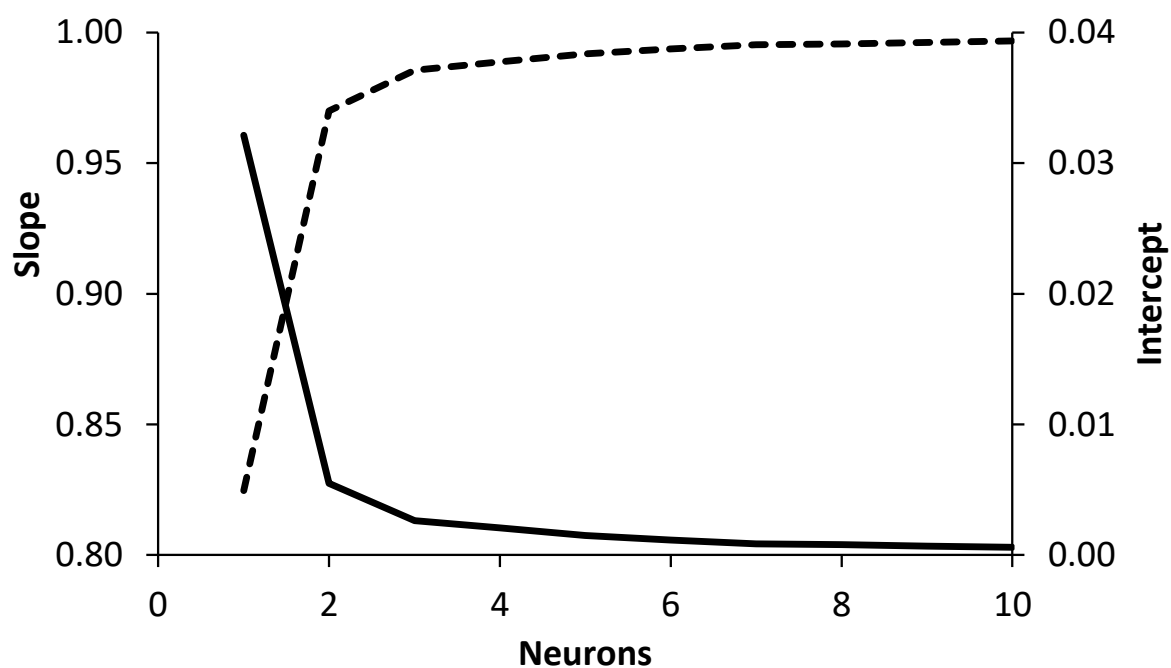


449

450

451 **Figure 1.** Test error as a function of the number of neurons in the hidden layer for (a) subtilisin and
452 (b) trypsin. Test errors reported as average of 30 trials trained by gradient descent with momentum
453 (solid line), resilient backpropagation (dotted line) and Levensberg-Marquardt algorithm (dashed
454 line).

(a)



(b)

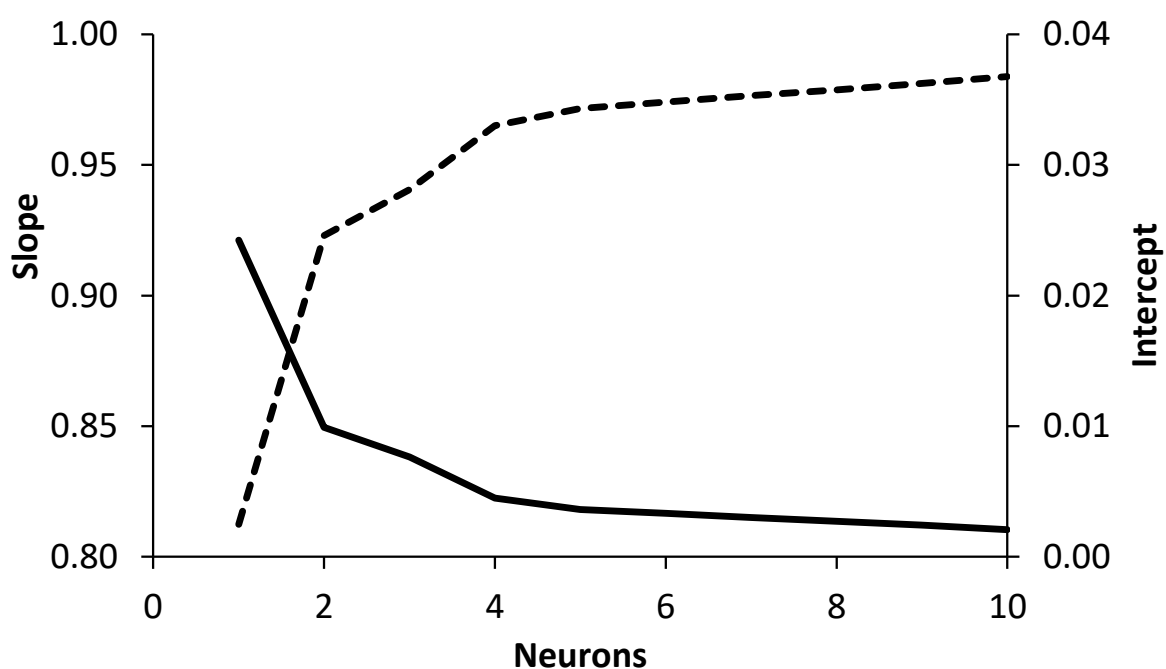
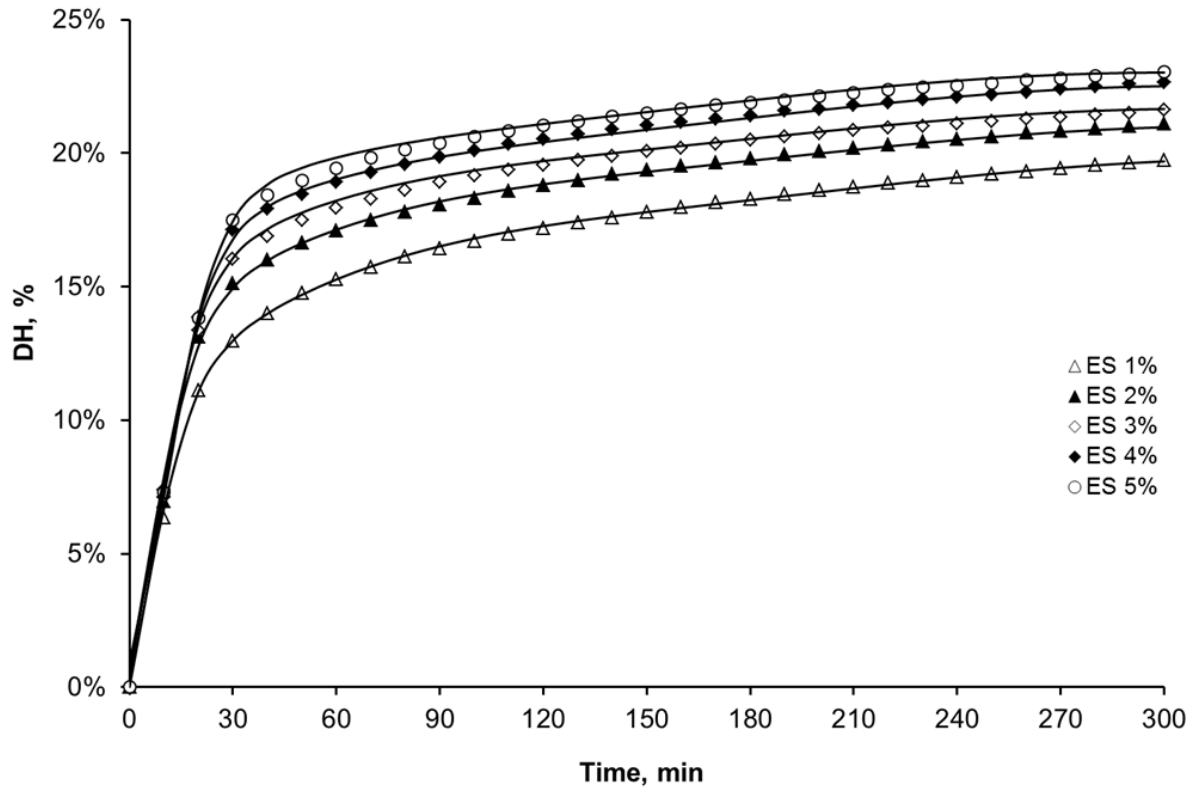


Figure 2. Slope (dashed line) and intercept (solid line) of the linear fit of experimental against calculated DH as a function of the number of neurons in the hidden layer for (a) subtilisin and (b) trypsin. Slope and intercept reported as average of 30 trials trained by the Levenberg-Marquardt algorithm.

(a)



(b)

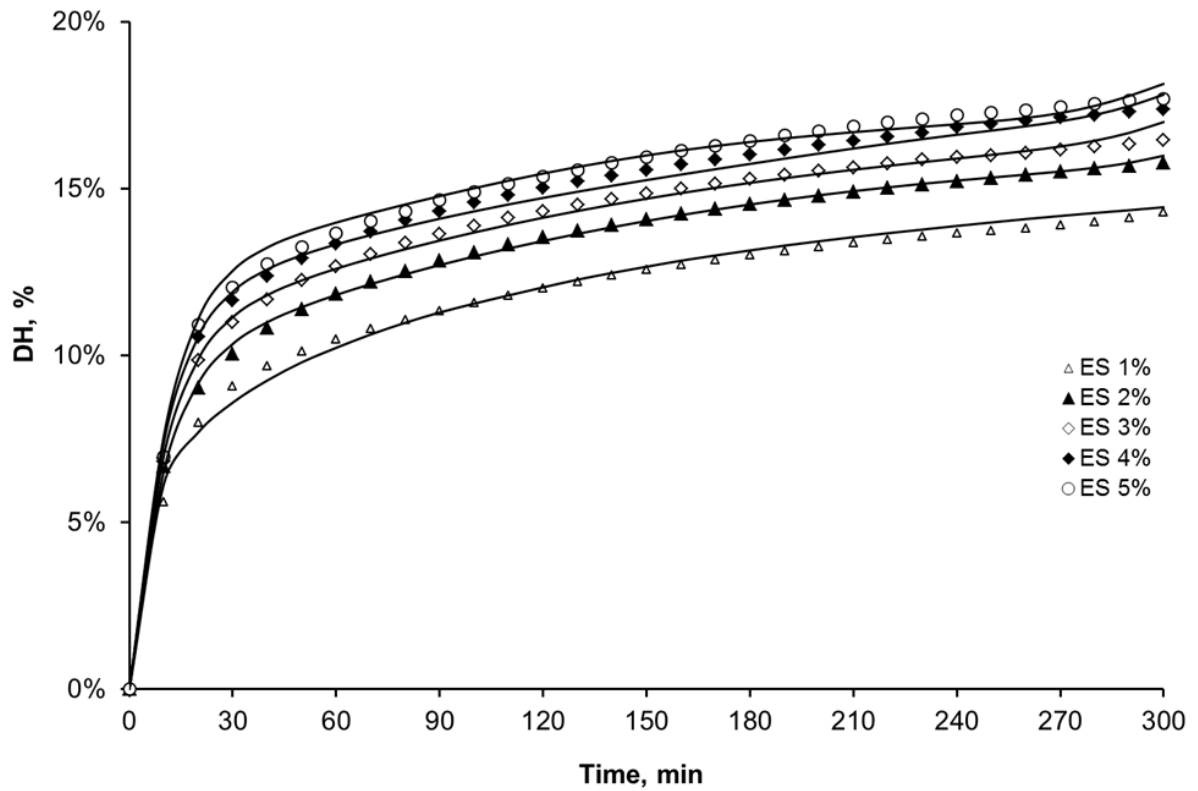
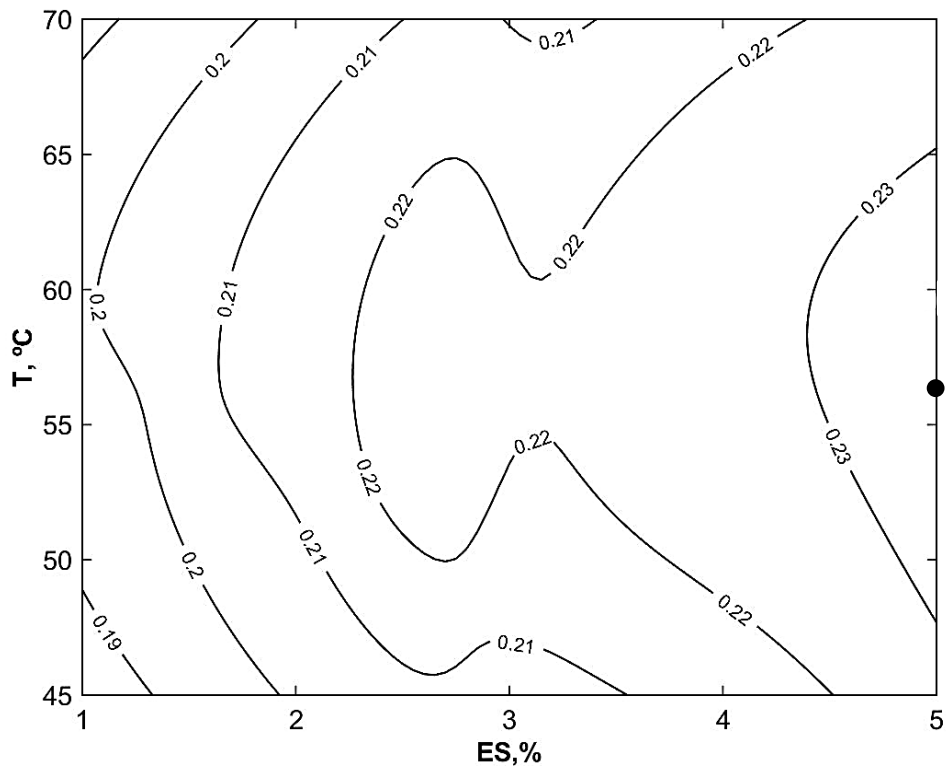


Figure 3. Experimental (marker points) and predicted (solid lines) values of DH against time of reaction and enzyme-substrate ratio for (a) subtilisin at 50°C and (b) trypsin at 50°C.

(a)



(b)

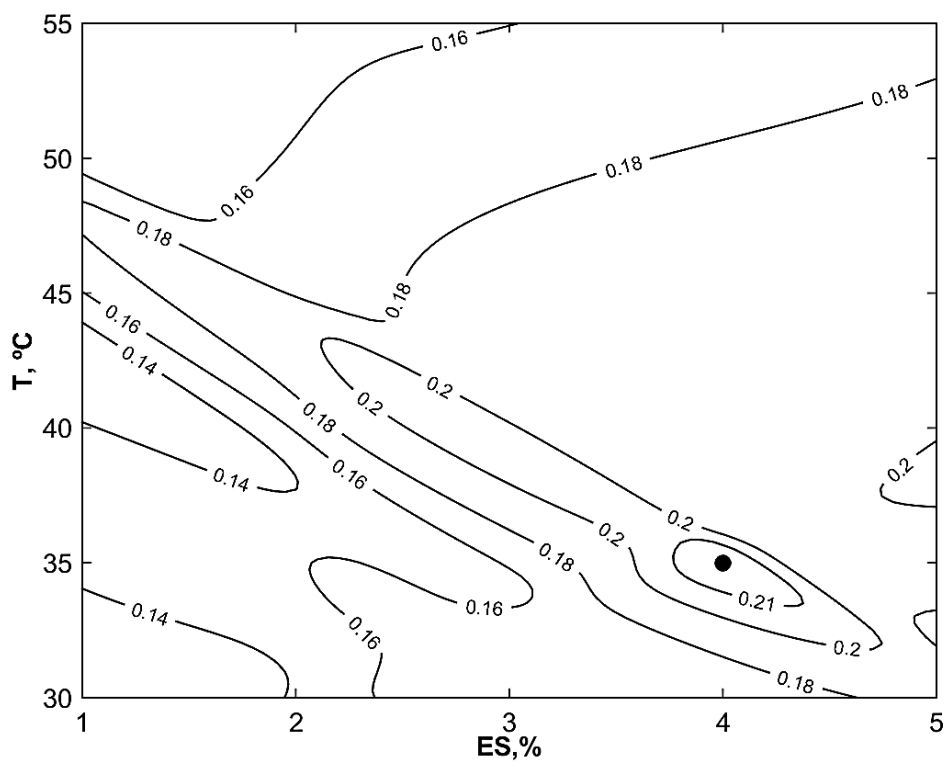


Figure 4. Contour plots of final DH (5 h) against enzyme-substrate ratio and reaction temperature for (a) subtilisin ANN model with 8 neurons in the hidden layer and (b) trypsin ANN model with 10 neurons in the hidden layer.

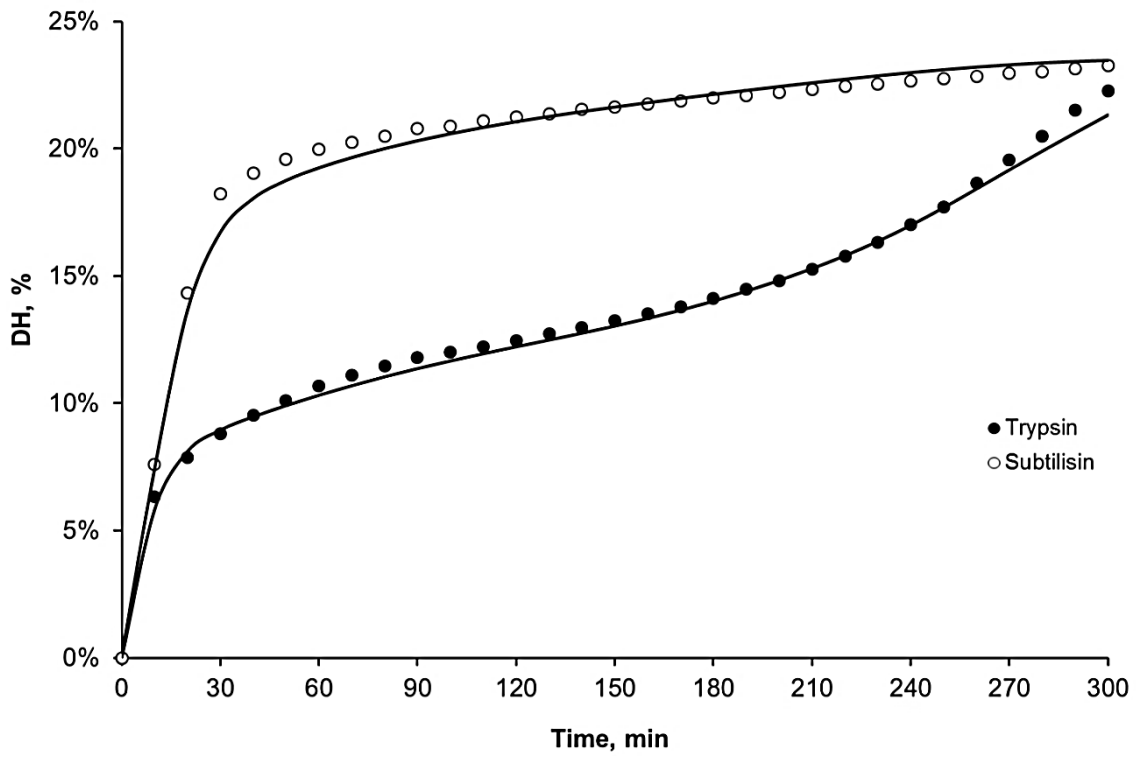


Figure 5. Validation experiment: experimental (marker points) and predicted (solid lines) values of DH against time of hydrolysis under optimal conditions for maximising DH (ES 5% , T=56.4°C and ES 4%, T = 35°C for subtilisin and trypsin, respectively).